Mathematical Modelling and Design of an Advanced Once-Through Heat Recovery Steam Generator

Marie-Noëlle Dumont [1], Georges Heyen
LASSC, University of Liège, Sart Tilman B6A, B-4000 Liège (Belgium)

Abstract

The once-through heat recovery steam generator design is ideally matched to very high temperature and pressure, well into the supercritical range. Moreover this type of boiler is structurally simpler than a conventional one, since no drum is required.

In a conventional design, each tube plays a well-defined role: water preheating, vaporisation, superheating. Empirical equations are available to predict the average heat transfer coefficient for each region. For once-through applications, this is no more the case and mathematical models have to be adapted to account for the disappearance of the conventional economiser, boiler and superheater. General equations have to be used for each tube of the boiler, and the actual heat transfer condition in each tube has to be identified. The mathematical complexity as well as the number of equations is increased. A thermodynamic model has been selected and implemented to suit very high pressure (up to 240 bar), sub- and supercritical steam properties. Model use is illustrated by two case studies : a 180 bar once-through boiler (OTB) and a conventional boiler superheater and reheater.

Keywords :Once-through boiler; heat recovery steam generator (HRSG); water flow pattern

[1] Corresponding authors. Tel:+32 4 366 35 23 Fax: +32 4 366 35 25 ; E-mail address: MN.Dumont@ulg.ac.be

1. Introduction

Nowadays combined cycle (CC) power plants become a good choice to produce energy, because of their high efficiency and the use of low carbon content fuels (e.g. natural gas) that reduces the greenhouse gases production. CC plants couple a Brayton cycle with a Rankine cycle. The hot exhaust of the gas turbine (Brayton cycle) delivers energy to produce high-pressure steam for the Rankine cycle. The equipment where the steam production takes place is named the heat recovery steam generator (HRSG).

High efficiency in CC (up to 58%) can be achieved for two main reasons:

1. Improvements in the gas turbine technology (i.e. higher inlet temperature);
2. Improvement in the HRSG design

We focus here on the second point. The introduction of several pressure levels with reheat in the steam cycle in the HRSG allows recovering more energy from the exhaust gas (usually available between 600°C and 700°C). Exergy losses decrease, due to a better matching of the gas-cooling curve with the water/steam curve in the heat exchange diagram (Dechamps, 1998). Going to supercritical pressure with the OTB technology is another way to better match those curves and thus improve the CC efficiency.

New improvements are announced in near future to reach overall cycle efficiency as high as 60%.

In the present work we propose a mathematical model for the simulation and design of the once-through boiler. The modelling approach used for the simulation of a conventional boiler has to be revised, since the heat transfer regime in each tube can not be fixed by the equipment design. General equations have to be used for each tube of the boiler. Moreover there is a more significant evolution of the water/steam flow pattern type due to the complete water vaporization inside the tubes (in a conventional boiler, the circulation flow is adjusted to reach a vapour fraction between 20% and 40% in the tubes and the vapour is separated in the drum).

Changes of flow pattern induce a modification in the evaluation of the internal heat transfer coefficient as well as in the pressure drop formulation. The right equation has to be selected dynamically according to the flow conditions prevailing in the tube.

The uniform distribution of water among parallel tubes of the same geometry subjected to equal heating is not ensured from the outset but depends on the pressure drop in the tubes.

The disappearance of the drum introduces a different understanding of the boiler's behaviour.

Effects of the various two-phase flow patterns have to be mathematically controlled.

2.Thermodynamic model

To estimate water and steam properties, we make use of "IAPWS Industrial Formulation for the Thermodynamic Properties of Water and Steam" (Wagner et al, 1998). It replaces the previous industrial standard IFC-67. This formulation provides a very accurate representation of the thermodynamic properties of water and steam over a wide range of temperature and pressure with a formulation that is designed for fast computation.

The IAPWS Industrial Formulation 1997 consists of a set of equations for different regions that cover the following range of validity:

$0°C < T < 800°C \quad p<1000$ bar

$800°C < T < 2000°C \quad p<100$ bar

Figure 1 shows the 5 regions into which the entire range of validity of IAPWS-IF97 is divided.

3. Mathematical Model

The model described hereafter should be applied to horizontal tube bundles (boilers with vertical gas path, figure 6 shows a typical tube layout). It has been developed for once through boilers but could also be used with conventional boiler. The complete set of equations developed here after has to be applied to each tube row or part of tube row of the complete tube bundle (for a tube bundle with 50 rows of tubes, the set has to be applied at least 50 times).

3.1. Heat transfer

3.1.1. Water side

Heat transfer equations must be formulated for steady state, forced flow through tubes. Mathematical models for conventional boilers are usually based on empirical equations corresponding to each region of the boiler: the economizer, the boiler and the superheater. Those three parts of boiler are clearly separated thus it is not difficult to choose the appropriate equation. In a once-through boiler this separation is not so clear. We have first to estimate the flow pattern in the tubes, and on this basis to select the appropriate heat transfer equation. “Liquid single phase” and “vapour single phase” conditions are easily identified from temperature and pressure data. According to Gnielinski (1993) the equation 1 applies for turbulent and hydrodynamically developed flow.

$$Nu = \frac{(\xi/8)\left(\mathrm{Re}_l - 1000\right)\mathrm{Pr}}{1 + 12{,}7\sqrt{(\xi/8)}\left(\mathrm{Pr}^{2/3} - 1\right)} = \frac{\alpha * d}{\lambda} \; ; \; \xi = \frac{1}{\sqrt{\left(1{,}82\log_{10}\mathrm{Re} - 1{,}64\right)}} \qquad (1)$$

During vaporization different flow patterns can be observed, for which the rate of heat transfer also differs. In stratified-wavy flow pattern incomplete wetting has an effect on the heat transfer coefficient. A reduction appears for this type of flow pattern. Computing conditions where a change in flow pattern occurs is useful. Steiner (1993) clearly exposed a method to establish a flow pattern map in horizontal tube for given pressure and flow conditions. This method has been used in this study. The different flow pattern in the vaporisation zone of the OTB are given in figure 2. The heat transfer coefficient is estimated from numerous data. It is a combination of convective heat transfer coefficient and nucleate boiling heat transfer coefficient.

$$\alpha(z)=\sqrt[3]{\alpha(z)_{conv}^{3}+\alpha(z)_{B}^{3}} \tag{2}$$

$$\left(\frac{\alpha(z)_{conv}}{\alpha_{lo}}\right)^{-2}=\left[(1-x)+1.2x^{0.4}(1-x)^{0.01}\left(\frac{\rho_{liq}}{\rho_{vap}}\right)^{0.37}\right]^{-2.2} + \left[\frac{\alpha_{go}}{\alpha_{lo}}x^{0.01}\left(1+8(1-x)^{0.7}\left(\frac{\rho_{liq}}{\rho_{vap}}\right)^{0.67}\right)\right]^{-2} \tag{3}$$

$$\alpha(z)_B=\psi*18418*\left(\frac{\dot{q}}{15*10^4}\right)^{n(p^*)}\left[2.692p^{*0.43}+\frac{1.6p^{*6.5}}{1-p^{*4.4}}\right] \cdot\left(\frac{0.01}{d}\right)^{0.5}\left(\frac{R_a}{10^{-6}}\right)^{0.133}\left(\frac{G}{100}\right)^{0.25}\left[1-p^{*\,0.1}\left(\frac{\dot{q}}{\dot{q}_{cr,PB}}\right)\right] \tag{4}$$

with

$$n=\kappa(0.8-0.13*10^{\left(0.66.p^*\right)}$$

$$\dot{q}_{cr,PB}=9.19*10^6\,p^{*\,0.4}\left(1-p^*\right)$$

$$p^*=\frac{p}{p_c}=\frac{p}{220.64}$$

The correction coefficients ψ and κ are functions of the heat conduction ($\lambda_w s$) of the tube wall. They have to be applied when ($\lambda_w s$) < 0.7 W/K, which is the case for HRSG (Table 1) For bubble flow, ψ is set to 1.

α_{LO} is the heat transfer coefficient with total mass velocity in the form of the liquid.

α_{GO} is the heat transfer coefficient with total mass velocity in the form of the vapour.

Evolution of the internal coefficients in a typical OTB is presented in figure 3.

32.1.2. Fumes side

The same set of equations can be used used for a conventional heat recovery boiler and a once trough heat recovery boiler. The main contribution to the heat transfer coefficient is due to convection, since the fumes temperature is rather low and the tube spacing is short. Radiative heat transfer plays a secondary role. The effect of the turbulence has been introduced to reduce the heat transfer coefficient in the first few rows of the tube bundle.

The main difficulty to evaluate the heat transfer coefficient for the fume side comes from the fins that enhance the heat transfer, but could also produce other sources of resistance in the heat transfer, such as fouling on the surface of fins or inadequate contact between the core tube and the fin base.

Several methods have been implemented in the model to evaluate the heat transfer coefficient on the gas side. Equation 6 is a general equation, which evaluates the Nusselt number in cross flow over pipes.

$$Nu_d = C \, \mathrm{Re}_d^m \left(\frac{A}{A_b} \right)^n \mathrm{Pr}^l \tag{6}$$

Values for parameters “C”, “m”, “n” and “l” are given in table 2.

Fins efficiency is estimated from following equations:

$$H_r = l_f \left(1 + \frac{e_a}{2 l_f} \right) \left(1 + 0.35 \ln \left(\frac{d_a}{d} \right) \right) \tag{7}$$

$$X = H_r \sqrt{\frac{2\alpha_f}{e_a \lambda_a}} \tag{8}$$

$$\eta_f = \frac{\tanh(X)}{X} \tag{9}$$

Finally an apparent heat transfer coefficient is computed from equation 10:

$$\alpha_{app} = \alpha_f * \left[\frac{A_{po}}{A} + \eta_f \frac{A_{fo}}{A} \right] \tag{10}$$

Some tube manufacturers supply specific correlations whose coefficients have been tuned to match extensive data for their specific tube design. For instance, the tube manufacturer ESCOA recommends (ESCOA, 1979):

$$\alpha_f = j * G * c_p * \mathrm{Pr}^{-2/3} \tag{11}$$

$$j = C_1 * C_3 * C_5 * (\frac{d_a}{d})^{0,5} * (\frac{T_b}{T_s})^{0,25} \tag{12}$$

For solid fins and staggered arrangement for tubes :

$$C_1 = 0,25\,\mathrm{Re}^{-0,35} \tag{13}$$

$$C_3 = 0,35 + 0,65 e^{(-0,25 l_f / s_f)} \tag{14}$$

$$C_5 = 0,7 + \left[0,7 - 0,8 e^{(-0,15 N_r^2)} \right] * \left[e^{(-lp/tp)} \right] \tag{15}$$

3.1.3. Overall heat transfer coefficient

Finally the overall heat transfer coefficient is obtained from equation 16.

$$\frac{1}{\alpha} = \frac{1}{\alpha_{app}} + \frac{e}{\lambda * \frac{A_w}{A}} + \frac{1}{\alpha_i * \frac{A_i}{A}} \tag{16}$$

The overall heat transfer for each tube is computed with:

$$Q = \alpha * A * \Delta T_{sl} \tag{17}$$

We call ΔT_{sl} “semi logarithmic temperature difference” (equation 18). It is the best compromise between pure logarithmic temperature difference that has no sense here (only one tube) and pure arithmetic temperature difference that does not allow following the evolution of water properties along the tube.

$$\Delta T_{sl} = \frac{\left(T_{w2} - T_{w1}\right)}{\ln\left[\left(T_{mf} - T_{w1}\right) \Big/ \left(T_{mf} - T_{w2}\right)\right]} \tag{18}$$

$$T_{mf} = \frac{T_{f1} + T_{f2}}{2} \tag{19}$$

The heat exchange diagram of a typical OTB is presented in figure 4.

3.2. Pressure drop

3.2.1. Water side

Water flows in several parallel channels, submitted to slightly different heating patterns, thus the flows distribution will be influenced by pressure drops.

$$\Delta P = \frac{f \cdot \rho \cdot \overline{V}^2}{2g} \frac{l}{d_i} \quad \text{with} \quad \begin{cases} f = \dfrac{64}{\mathrm{Re}} & \text{(laminar)} \\ f = \dfrac{0.3164}{\sqrt[4]{\mathrm{Re}}} & \text{(turbulent)} \end{cases} \tag{20}$$

The coefficient f depends on the Reynolds number for flow within the tube. In laminar flow, the Hagen-Poiseuille law can be applied. In turbulent flow the Blasius equation is used. The main difficulty is the evaluation of water pressure drop during transition boiling. The pressure drop consists of three components: friction (ΔP_f), acceleration (ΔP_m) and static pressure (ΔP_g). In once-through horizontal tubes boiler ΔP_g=0. The Lockard-Martinelli formulation is used to estimate the friction term.

$$\left[\frac{\Delta P}{L}\right]_{2\,phases} = \left[\frac{\Delta P}{L}\right]_{liquid} \cdot \Phi^2_{ftt} \tag{21}$$

$$\Phi^2_{ftt} = 1 + \frac{20}{X} + \frac{1}{X^2} \tag{22}$$

$$X=\sqrt{\frac{\left[\Delta P/L\right]_{liquid}}{\left[\Delta P/L\right]_{vapor}}}=\left(\frac{1-x}{x}\right)^{0,875}\left(\frac{\rho_{go}}{\rho_{lo}}\right)^{0,5}\left(\frac{\eta_{lo}}{\eta_{go}}\right)^{0,125} \tag{23}$$

The acceleration term is defined with equation 24 where ε is the volume fraction of vapour (void fraction defined by equation 25).

$$\Delta P_m = G^2 * \left|\frac{x^2}{\varepsilon * \rho_{vap}} + \frac{(1-x)^2}{(1-\varepsilon) * \rho_{liq}}\right|_{x_1}^{x_2} \tag{24}$$

$$\varepsilon = \frac{x}{\rho_g}\left[\left(1+0.12(1-x)\right)\left(\frac{x}{\rho_g}+\frac{1-x}{\rho_l}\right)+\frac{1.18(1-x)\left[g\sigma\left(\rho_l-\rho_g\right)\right]^{0.25}}{G_{tot}\rho_l^{0.5}}\right]^{-1} \tag{25}$$

It is recommended to discretize each tube in several short sections in order to obtain more accurate results. Figure 5 shows local pressure drop evolution in a tube, as calculated by this model. The main pressure drop is observed where vaporisation takes place.

3.2.2. Fumes side

The pressure drop in a tube bundle is given by equation 26. In this case the number of rows (N_R) plays an important role in the pressure drop evaluation. For solid fins and staggered arrangement for tubes, the ESCOA correlation has been selected (ESCOA, 1979):

$$\Delta P = \frac{(f+a)\cdot G^2 N_r}{\rho_b} \tag{26}$$

$$a = \left[\frac{1+\beta^2}{4N_r}\right]\rho_b\left[\frac{1}{\rho_2}-\frac{1}{\rho_1}\right] \tag{27}$$

$$\beta = \frac{A_n}{A_d} \tag{28}$$

$$f = C_2 * C_4 * C_6 * \left(\frac{d_a}{d}\right)^{0.5} \tag{29}$$

$$C_2 = 0,07 + 8\,\mathrm{Re}^{-0,45} \tag{30}$$

$$C_4 = 0,11\left[0,05\frac{tp}{d}\right]^{(-0,7(l_f/s_f)^{0,2})} \tag{31}$$

$$C_6 = 1,1+\left[1,8-2,1e^{(-0,15N_r^2)}\right]*\left[e^{(-2lp/tp)}\right] - \left[0,7-0,8e^{(-0,15N_r^2)}\right]*\left[e^{(-0,6lp/tp)}\right] \tag{32}$$

4. Examples

The following examples are based on CMI boilers design. CMI Utility Boilers is a company active in the design, construction, erection and commissioning of heat recovery boilers associated with high capacity gas turbines used in combined cycle power plant.

4.1.Once through boiler

The once through HRSG design features are:

- Vertical gas path.
- Economizer and vaporizer are combined (no intermediate header).
- Water is flowing down from top to bottom in countercurrent arrangement.
- Ready to work with the latest generation of gas turbines.
- Fuel can be natural gas, distillate, heavy oil or crude oil.

Results have been obtained for an OTB of pilot plant size presented in figure 6. Main design parameters of the steam generators is given in tables 3 and 4.

The simulation model has been implemented in VALI software (BELSIM, 2002). Each tube or tube section can be represented by a separate simulation object. The graphical user interface allows easy modification of the tube connections and the modeling of multiple pass bundles (figure 8).The simulation of the OTB described here is performed by connecting at least 42 modules, one for each tube row. Since VALI implements a numerical procedure to solve large sets of non-linear equations, all model equations are solved simultaneously. Convergence is smooth and is achieved in a few iterations (figure 7).

4.2. Conventional boiler and reheater

Other results were obtained for a superheater and a reheater of a conventional boiler. Boiler description is given in table 5.

This allowed comparison of the detailed modelling presented here, with the more global design approach that has been applied previously.

Although our design tool has been developed to model once through boilers, there is no limitation and it can also be applied to model conventional boiler. Figure 3 compares the predicted evolution of heat transfer coefficient in each tube, with average values predicted with the design procedures applied in the past.

Economiser and vaporiser are well described with traditional empirical equations however the extra modelling work required by the new method provides interesting information for superheater and reheater.

The example shown here allowed to understand some failures in the tubes of a super heater. Figure 9 clearly shows that the fumes temperatures (shown in italic) does not evolve homogeneously in the boiler. Gas temperature may vary by more than 30° across the flue channel. Water temperature profiles also differ for parallel tubes thus pressure drops patterns also differ. In order to balance the pressure drop in parallel tubes, the water flow rate has to differ. The heat transfer might become degraded in some tubes, which results in overheating and increases the risk of failure.

The module is now used during the design to analyse the water temperature profile when selecting between alternative tube patterns.

5. Conclusions and Future Work

The mathematical model of the once-through boiler has been used to better understand the behaviour of the boiler. Future mathematical developments have still to be done to improve the OTB design. The criteria for flow stability have to be reviewed since it is certainly different in an OTB design or in an assisted circulation boiler design. Automatic generation of alternative bundle layouts in the graphical user interface is also foreseen.

6. Acknowledgements

CMI Utility boilers (Belgium) has financially supported this work, and provided design data for the examples.

7. Nomenclature

A	total area of outer surface (m²)
A_b	bare tube outside surface area
A_{fo}	fin outside surface area (m²)
A_i	inside surface area (m²)
A_{po}	free area of tube outer surface
A_w	mean area of homogeneous tube wall
c_p	specific heat capacity at constant pressure (J/kg/K)
d_i	tube internal diameter (m)
d	tube external diameter (m)
d_a	fin diameter (m)
e_a	fin thickness (m)
ΔP	pressure drop
f	pressure drop coefficient
g	acceleration due to gravity (m²/s)
G	mass flux (kg/m^2/s)
H	enthalpy flow (kW)
l_f	fin height = $(d_a$-$d)/2$ (m)

lp	longitudinal tube pitch (m)
tp	transverse tube pitch (m)
Nu	Nusselt number $Nu_l = \frac{\alpha \cdot l}{\lambda}$
N_r	number of rows in the direction of flow
P	pressure (bar)
Pr	Prandl number $\Pr = \frac{c_p \cdot \eta}{\lambda}$
Q	exchanged heat (kW)
$\dot{q}$	heat flux (W/m²)
Re	Reynolds number $\mathrm{Re}_d = \frac{G * d}{\eta}$
Ra	Arithmetic mean roughness height (m)
s_f	fin spacing (m)
T	temperature (K)
T_s	average fin surface temperature (K)
T_b	average outside fluid temperature (K)
$\overline{V}$	fluid velocity (m/s)
x	vapour mass fraction
x_i	component flow rate (kg/s)
α	heat transfer coefficient (kW/m²/K)
α_f	external (fumes side) heat transfer coefficient (kW/m²/K)
α_i	internal (water side) heat transfer coefficient (kW/m²/K)
$\alpha(z)$	local heat transfer coefficient
ε	volume fraction of vapor

λ thermal conductivity (W/m/K)

λ_a fin thermal conductivity (W/m/K)

ρ density (kg/m^3)

η dynamic viscosity (Pa.s) or (kg/m/s)

η_f fin efficiency

8. References

BELSIM (2002) VALI III users guide, Belsim s.a., Saint-Georges-sur-Meuse, Belgium

Dechamps, P.J. (1998), Advanced combined cycle alternatives with the latest gas turbines, ASME J. Engrg. Gas Turbines Power 120, 350–35

ESCOA (1979), Fin Tube Manual, ESCOA corp.

Gnielinski, V. (1993), *VDI heat atlas*, GA,GB, VDI-Verlag, Düsseldorf, Germany

Rizhu, Li, Huaiming, Ju (2002), Structural design and two-phase flow stability test for the steam generator, Nuclear Engineering and Design 218, 179-187

Steiner, D. (1993) *VDI heat atlas*, VDI-Verlag, HBB, Düsseldorf, Germany

Wagner, W., Kruse (1998), Properties of Water and Steam / IAPWS-IF97, Springer-Verlag, Berlin, Germany

9. Figures

Figure 1 : IAPWS-IF97 range of validity

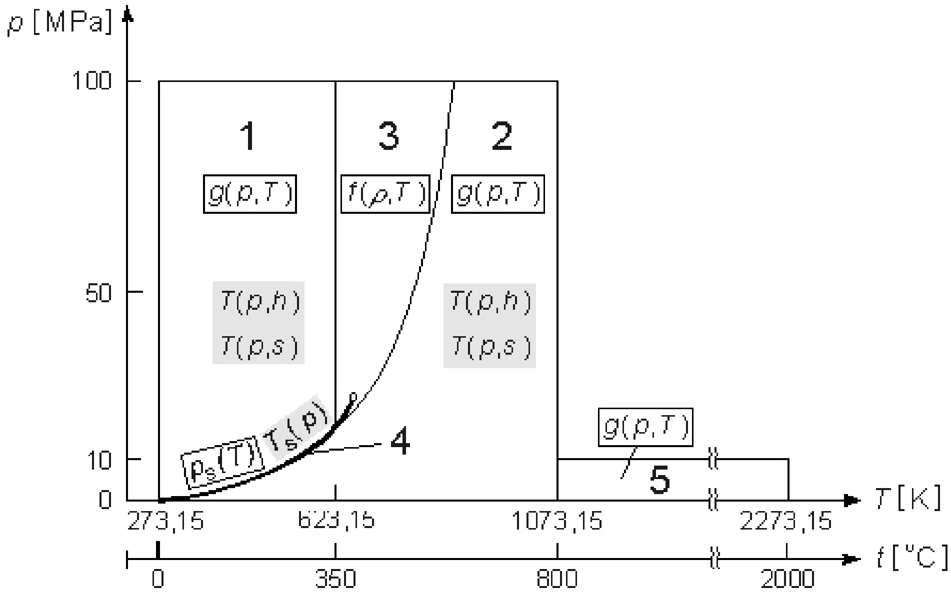

Figure 2 : Flow pattern in the boiling zone for horizontal flow (VDI,1993).

Dots show flow evolution in a typical OTB

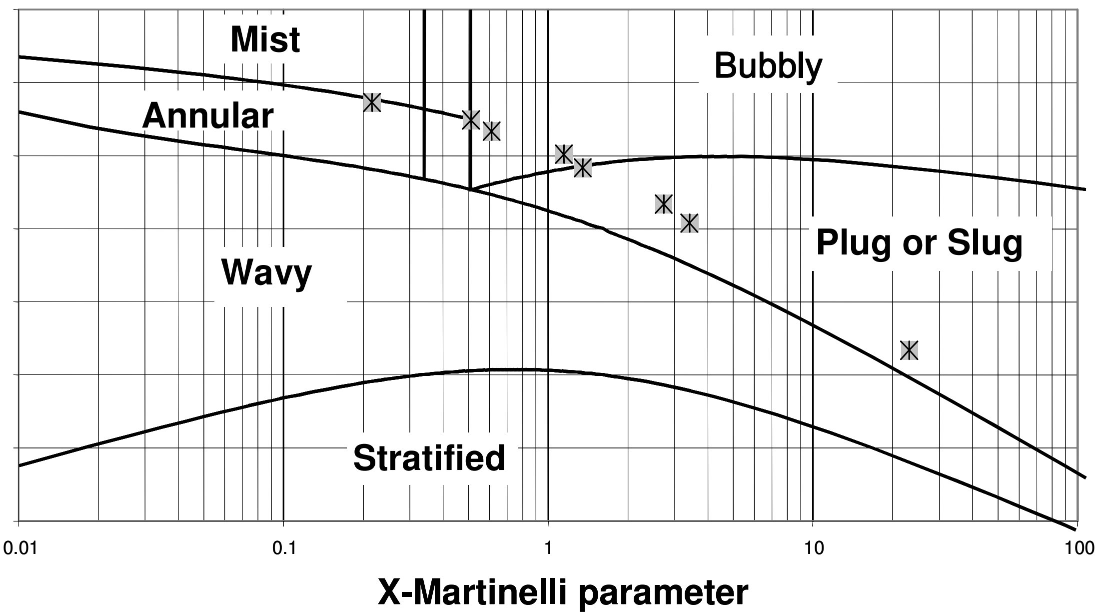

Figure 3 : Internal heat transfer coefficient evolution in the once through boiler compared to average coefficients of a conventional steam generator (large dots)

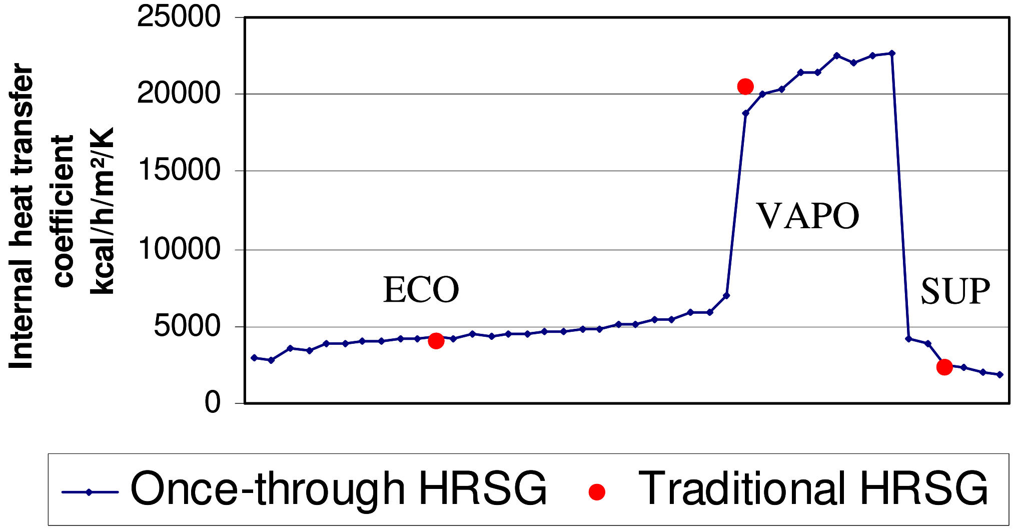

Figure 4 : Fumes and water temperature evolution through out the boiler with the "OTB" mathematical formulation

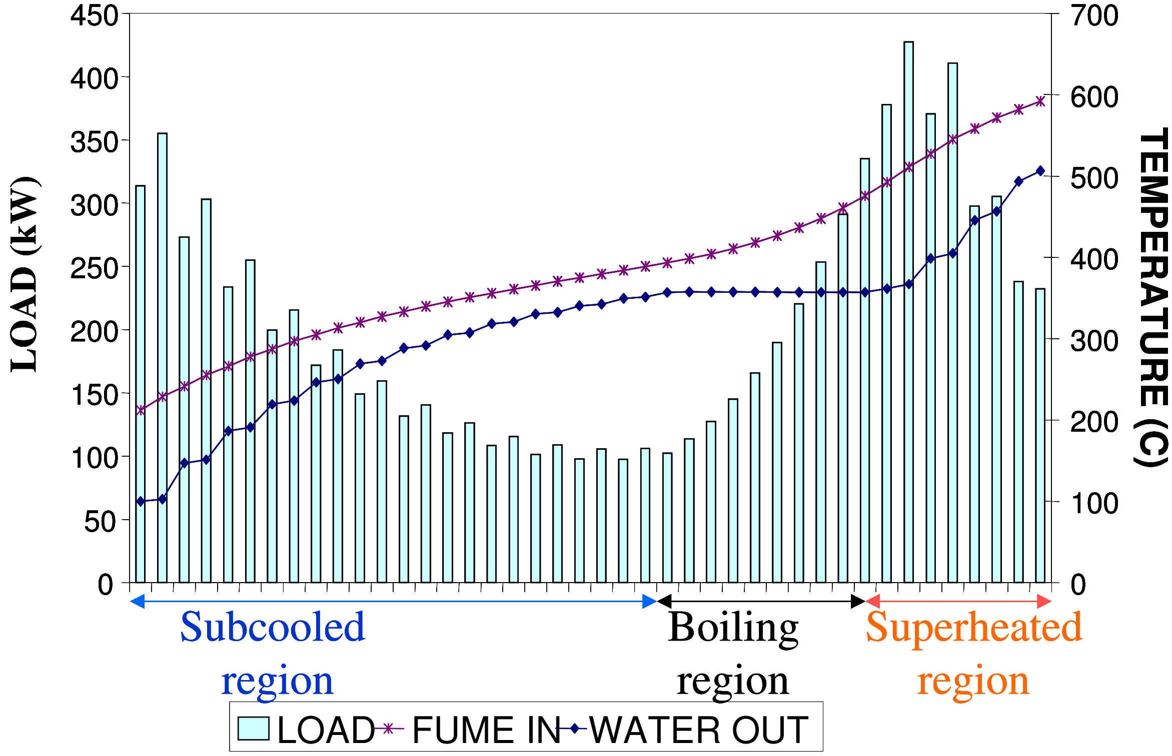

Figure 5 : local pressure drop evolution in a continuous flow path from inlet water to outlet superheated steam

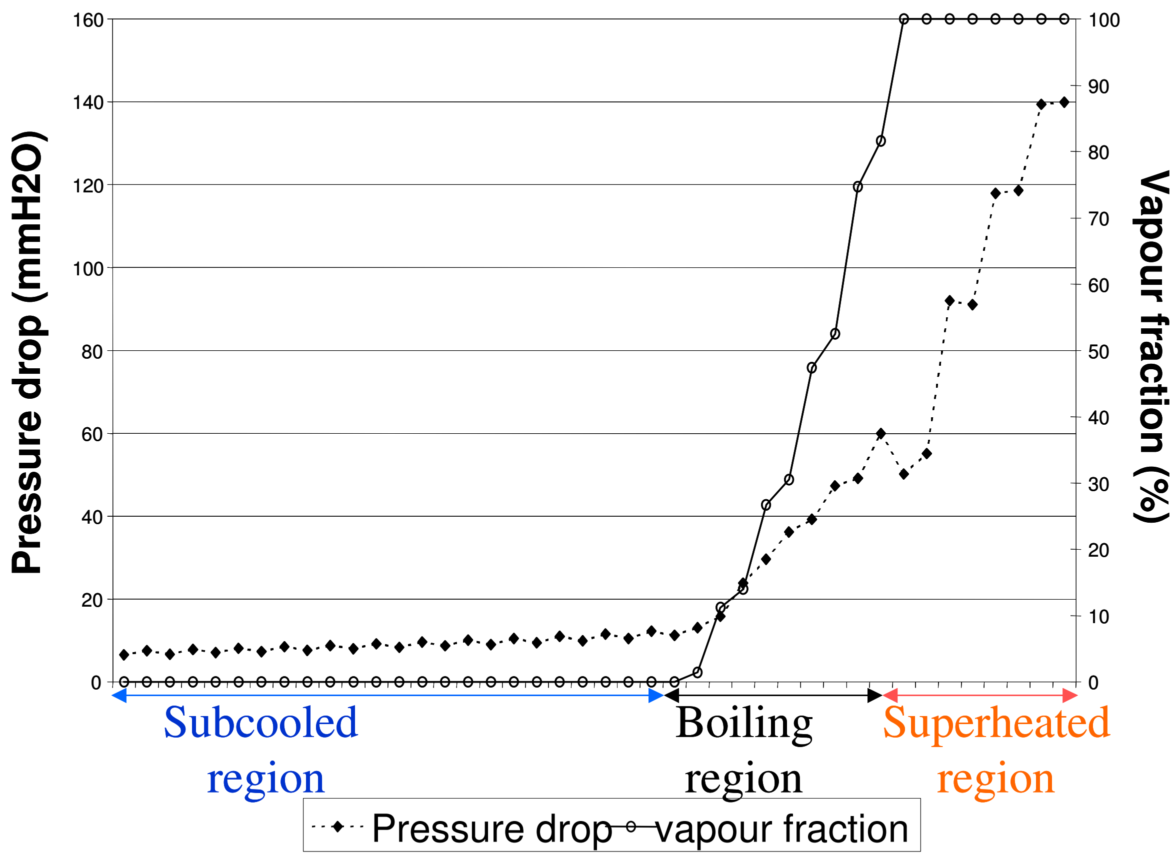

Figure 6 : Details of the pressure parts assembly of the once-through boiler

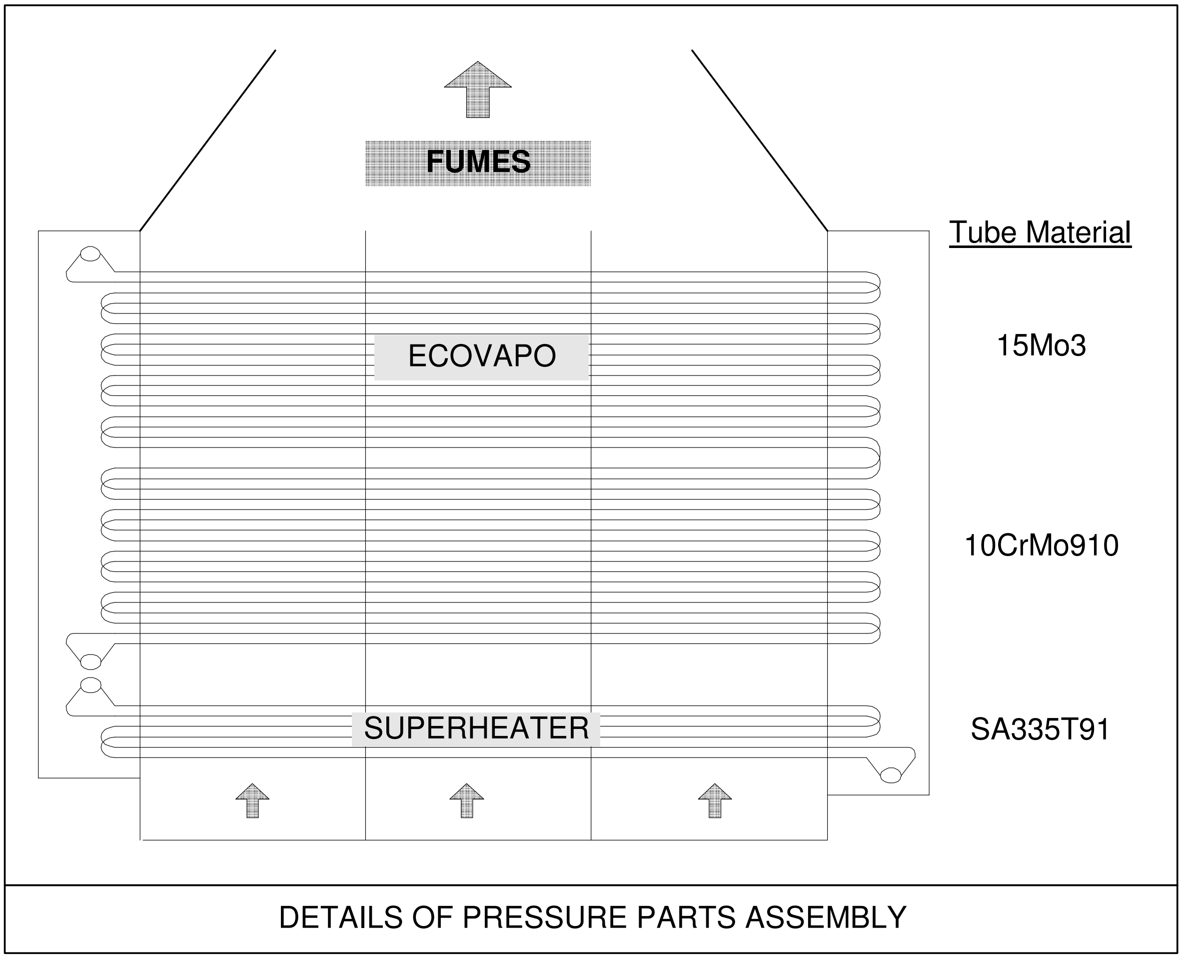

Figure 7: Convergence evolution for the OTB example

Settings	
File Name	aim.bls
Model	BOILER
Version	3.0
Mea File	
Tag File	
Flex File	
Options	-htm -sqp -dbg

Phase	INF	WRN	ERR	ERS	ERF	CPU
TAG Reading	0	28	0	0	0	0.040
Verification	0	0	0	0	0	0.980
Analysis	158	108	1	0	0	0.760
Resolution	0	0	0	0	0	39.590
Statistics	0	0	0	0	0	3.820
Report	0	0	10	0	0	1.170
Output	0	0	0	0	0	1.110

Analysis	
Number of equations	720
Number of unmeasured variables	713
Number of constants	95
Number of measured variables	27
Obvious number of redundancies	7
Total number of redundancies	28
Number of trivial redundancies	0

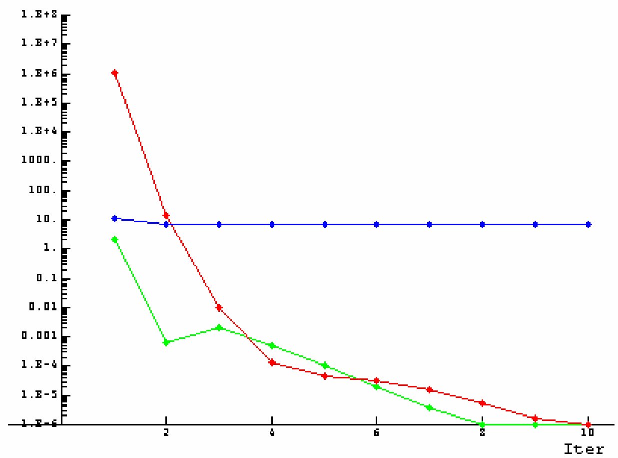

Resolution	
Iteration	10 / 100
Sum of square residues	0.29854E-06
Objective Function	7.3177
Chi-square	41.340
Number of active bounds	0
Flagged tags	0

Figure 8 : Bundle layout automatically generated with the appropriate connections in the graphical user interface of Vali software

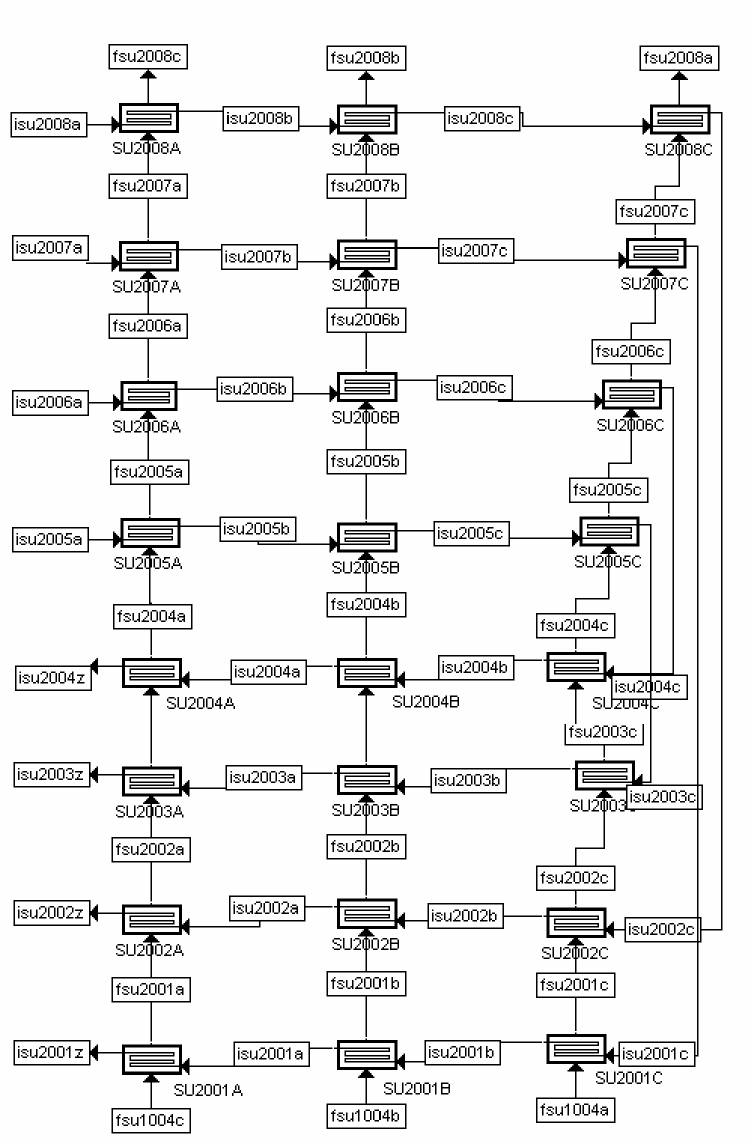

Figure 9 : Results obtained for a superheater and a reheater of a conventional boiler.

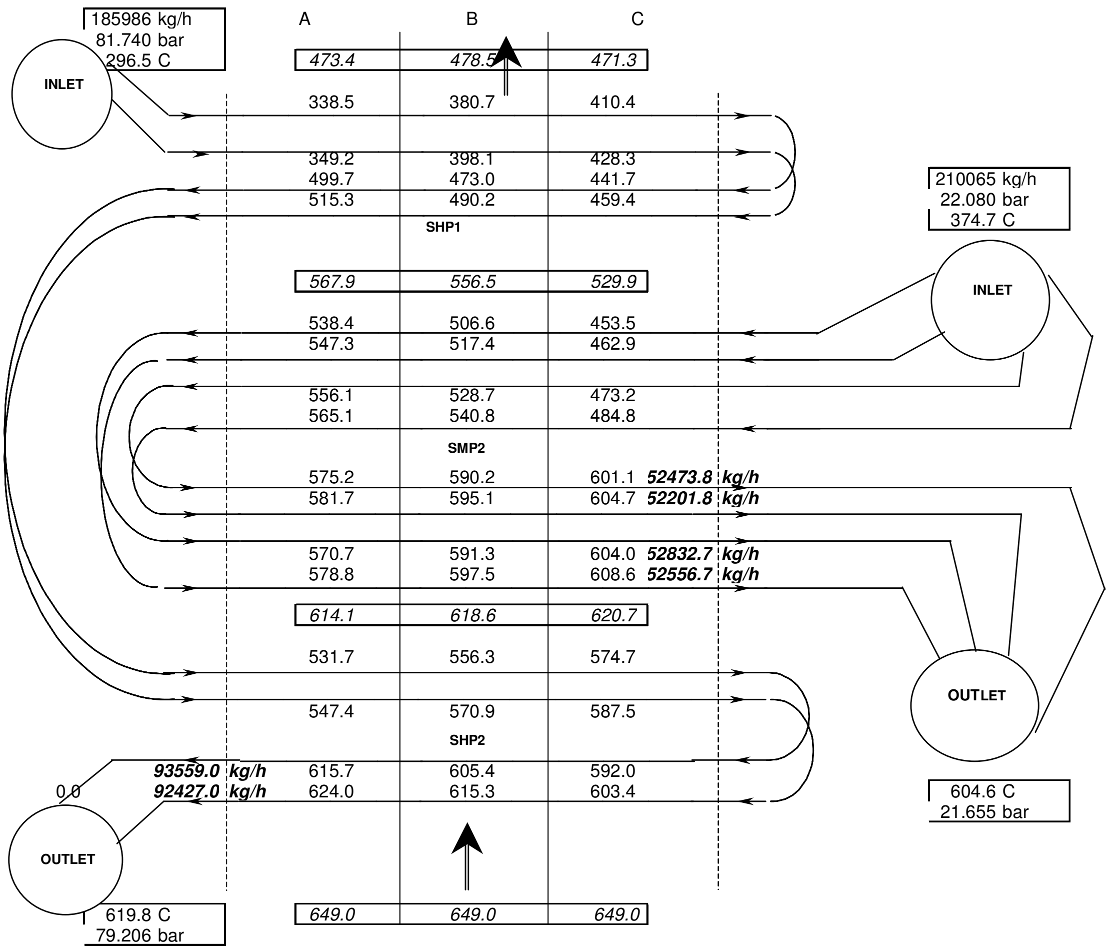

10.Tables

Table 1: correction coefficients for nucleate boiling heat transfer coefficient

	min value	max value	value for OTB example
κ	0.72	1	0.8
ψ (annular flow)	0.74	1	0.86
ψ (slug flow)	0.65	1	0.79
ψ (stratified and wavy flow)	0.45	0.86	0.61

Table 2: VDI coefficients for Nusselt correlation (fumes side)

VDI	C	m	n	l
In-line arrangement	0.22	0.6	-0.15	0.333
Staggered arrangement	0.38	0.6	-0.15	0.333

Table 3: OTB description

	ECOVAPO	SUPERHEATER
number of rows	36	6
tubes in parallel	2	2
tubes / row	13	13
tube diameter (d in m)	0.025	0.0269
tube thickness (m)	0.0029	0.0042
length (m)	6	6
fins /m	200	200
fin diameter (d_a in m)	0.049	0.049
transverse pitch (tp in m)	0.083	0.083
longitudinal pitch (lp in m)	0.073	0.073

Table 4: OTB operating conditions

	Flow rate (t/h)	Inlet temperature (C)	Outlet temperature (C)
WATER	10.25	44	500
FUMES	72.5	592	197

Table 5: conventional boiler description

	SUPERHEATER	REHEATER
number of rows	8	8
tubes in parallel	2	4
tubes / row	104	104
tube diameter (d in m)	0.038	0.0445
tube thickness (m)	0.0042	0.0033
length (m)	6.8	6.8
fins /m	290	285
fin diameter (d_a in m)	0.068	0.068
transverse pitch (tp in m)	0.091	0.091
longitudinal pitch (lp in m)	0.079	0.079
Tin water (°C)	296.5	374.7
Pin water (bar)	81.74	22.08
Tout water (°C)	619.8	604.6
Flow rate water (t/h)	185.986	210.065